CEP Clin Exp Pediatr Vol. 68, No. 8, 616–619, 2025
https://doi.org/10.3345/cep.2025.00360

Clinical note

Expanding genotype-phenotype correlation of Kenny-Caffey syndrome type 1

Manuela Lo Bianco, MD[1], Federica Sipala, MD[2], Xena Giada Pappalardo PhD[3,4], Gaia Fusto, MSc[3], Roberta Rizzo, MSc[5], Federico Favata, MD[6], Carla Cimino, MD[7], Silvia Marino, MD[8], Martino Ruggieri, BA, MD, PhD[1], Agnese Suppiej, MD, PhD[9], Simone Ronsisvalle, MSc, PhD[2], Raffaele Falsaperla, MD, PhD[9]

[1]Unit of Pediatric Clinic, Department of Clinical and Experimental Medicine, University of Catania, Catania, Italy; [2]Department of Drug Sciences, University of Catania, Catania, Italy; [3]Department of Biomedical and Biotechnological Sciences (BIOMETEC), Section of Pharmacology, University of Catania, Catania, Italy; [4]National Council of Research, Institute for Research and Biomedical Innovation (IRIB), Unit of Catania, Catania, Italy; [5]Endocrinology Section, Department of Clinical and Experimental Medicine, University of Catania, Garibaldi-Nesima Hospital, Catania, Italy; [6]Postgraduate Training Program in Pediatrics, Department of Clinical and Experimental Medicine, University of Catania, Catania, Italy; [7]Neonatal Intensive Care Unit and Neonatal Accompaniment Unit, Azienda Ospedaliero-Universitaria Policlinico Rodolico-San Marco, San Marco Hospital, University of Catania, Catania, Italy; [8]Unit of Pediatrics and Pediatric Emergency, Azienda Ospedaliero-Universitaria Policlinico Rodolico-San Marco, San Marco Hospital, Catania, Italy; [9]Department of Medical Science-Pediatrics, University of Ferrara, Ferrara, Italy

Kenny-Caffey syndrome type 1 (KCS1; OMIM#244460) is a rare autosomal recessive disorder, primarily reported in the Middle East among consanguineous families and caused by mutation in the *TBCE* gene (tubulin specific chaperone E; OMIM#604934) encoding a chaperone essential for microtubule assembly[1)] linked to the hearing loss.[2,3)] KCS1 is characterized by congenital hypoparathyroidism, hypocalcemia, growth retardation, microcephaly, delayed fontanelle closure, dysmorphic features, skeletal, dental and ocular abnormalities, renal complications (hypercalciuria, nephrocalcinosis), and endocrine dysfunctions (low insulin-like growth factor 1, growth hormone, insensitivity, hypothyroidism).

We report a female infant diagnosed with KCS1 through clinical exome sequencing (CES), which identified a homozygous pathogenic *TBCE* variant (rs767004810) inherited from heterozygous parents. Additional pathogenic variants were found in the *GJB2* gene (OMIM#121011) encoding connexin 26 (Cx26): a maternal frameshift (rs803389939) and a paternal missense (rs72474224), both in the only coding exon 2.[4)]

We employed a systems biology approach to assess clinical correlates (1) with structural and functional effects of *TBCE* and *GJB2* variants via inferring (2) a protein-protein interaction (PPI) network and (3) molecular dynamics simulations to explore shared disease path-

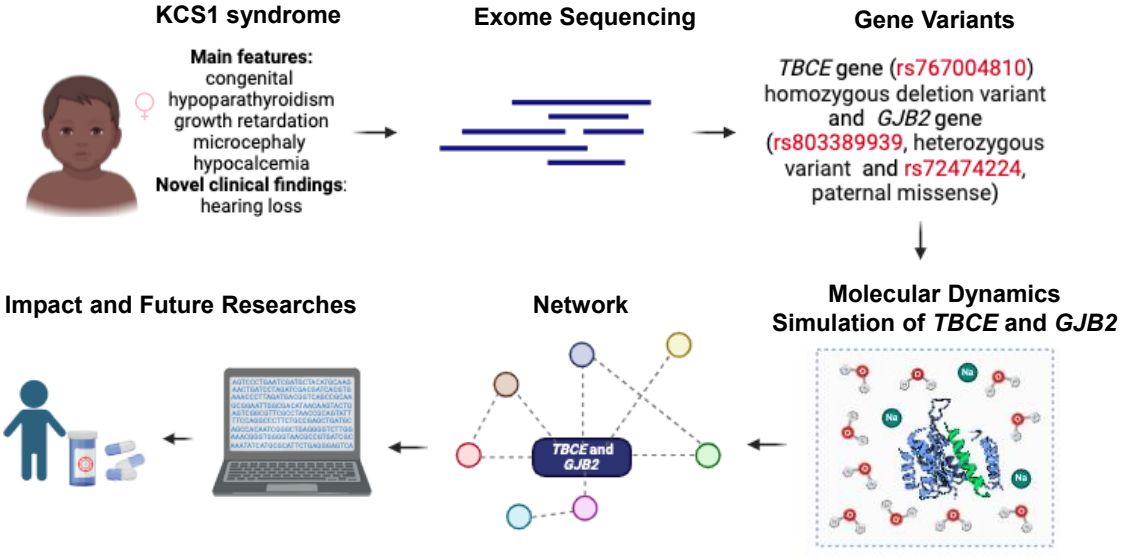

Graphical abstract. KCS1, Kenny-Caffey syndrome type 1.

Corresponding author: Raffaele Falsaperla. Department of Medical Science-Pediatrics, University of Ferrara, Ferrara, Italy
✉ Email: raffaele.falsaperla@unife.it, https://orcid.org/0000-0002-4482-3506
Received: 9 February 2025, Revised: 3 April 2025, Accepted: 21 April 2025

ways and expand the genotype-phenotype analysis (see more details in Supplementary material 1A and B).

(1) The patient was born at 38 weeks via spontaneous delivery to consanguineous African parents. Birth weight was 1,880 g (<1st percentile), length 43 cm (<1st percentile), and head circumference 30 cm (<1st percentile). Apgar scores were 9 and 10 at 1 and 5 minutes, respectively. In the first week, she experienced seizures due to severe hypocalcemia. Clinical examination showed axial and appendicular hypotonia, poor visual engagement, asymmetric Moro reflex, hyperreflexia, low-set ears, thin lips, small feet, and clinodactyly of the 3rd and 4th fingers. Additional findings included lower limb asymmetry, asymmetric thigh skin folds, right hip dislocation, left hip dislocatable (positive Barlow), and a nonpulsatile anterior fontanelle (4 cm×3 cm). Laboratory tests revealed anemia (hemoglobin, 6.6 g/dL), leukocytosis (white blood cell, 15,200 cells/μL), severe hypocalcemia (5.6 mg/dL), hyperphosphatemia (8.8 mg/dL), hypoparathyroidism (parathyroid hormone, 0.1 pg/mL), and elevated C-reactive protein (142 mg/L) and procalcitonin (1.08 ng/mL). Brain magnetic resonance imaging showed corpus callosum hypoplasia, enlarged frontotemporal subarachnoid spaces, and ventriculomegaly. Hip imaging confirmed stage 4 dysplasia with high dislocation on the left and stage 2b on the right. Treatment included intravenous calcium, oral magnesium and antibiotics administration, and blood transfusions, leading to biochemical normalization. At 6 months, ABR confirmed bilateral asymmetric hearing loss. The patient was discharged with a structured follow-up plan.

(2) The PPI network identified CRYGD, the γ-crystallin protein of eye lens, as a key connecting node between TBCE and GJB2, linking to the metallocarboxypeptidase CPN1 and another connexin, GJA3, as shown in Fig. 1. Of the 102-PPI network, only GJA3, CRYGD, and CPN1 form a functional link between TBCE and GJB2. This small but significant network segment helped correlate TBCE-GJB2 interactions with KCS1 features, suggesting potential novel disease markers.

(3) According to MSD findings, the mutant TBCE protein has an increased rigidity in the CAP-Gly domain, which disrupts the tubulin binding activity (Fig. 2A–D). In case of the mutant GJB2, the maternal variant affects the

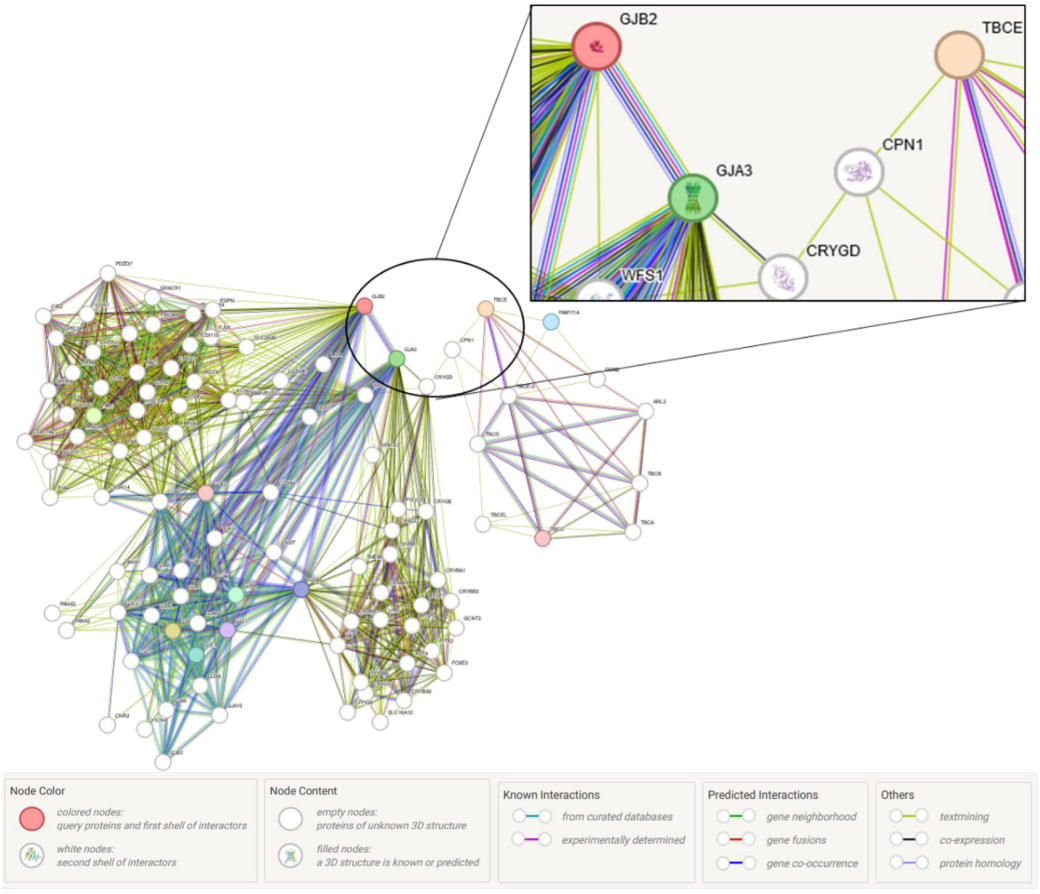

Fig. 1. Protein-protein interaction analysis of the *TBCE* and *GJB2* genes. Shared nearest-neighbor genes of *TBCE* and *GJB2* are clustered and zoomed. Network statistics: number of nodes, 102; number of edges, 1131; average node degree, 22.2; expected number of edges, 115; PPI enrichment *P* value: $<1.0^{e-16}$. (STRING permalink: https://version-12-0.string-db.org/cgi/network?networkId=b1NVqbgsaXx8).

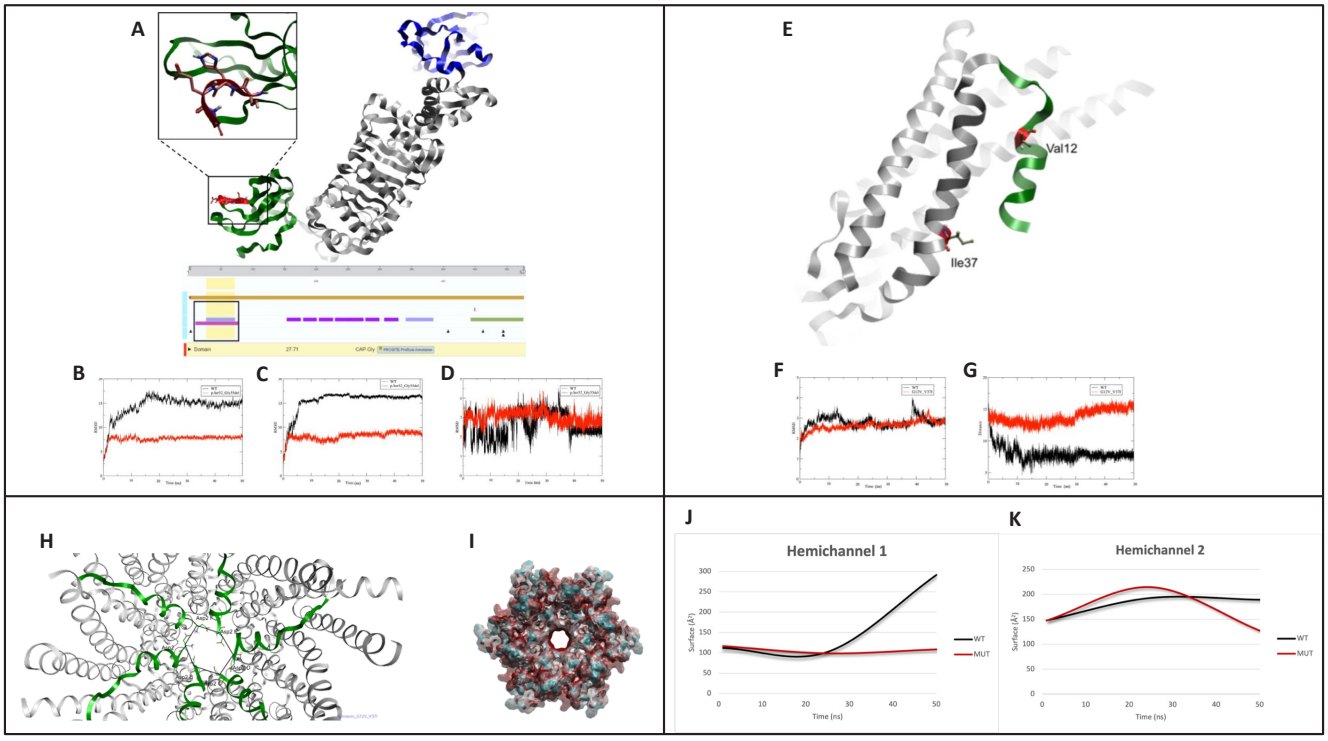

Fig. 2. (A) Structure of the wild-type TBCE protein. Above: Its UBL (blue), LRR (grey), and CAP-Gly (green) domains. The deletion of amino acids Ser52 to Gly55 caused by the rs767004810 variant is shown in red. Water and hydrogens were omitted for clarity. The frame was captured at 32 ns. Below: The black box indicates the region defined by Uniprot as the CAP-Gly spanning amino acids 27–71. CAP-Gly, cytoskeleton-associated protein, glycine-rich; RR, leucine-rich repeat; UBL, ubiquitin-like. (B-D) RMSD graphs of the WT and p.Ser52_Gly55del protein of TBCE during 50000 ps of simulation. (B) RMSD of the whole WT and mutated proteins. (C) RMSD of the WT and mutated UBL domains of the protein. (D) RMSD of the WT and mutated CAP-Gly domains of the protein. (E) Structure of subunit A of Cx26 with transmembrane domains (grey), NH-terminal domain (green), and mutated amino acids Val12 and Ile 37 (red). Water, hydrogens, and the membrane were omitted for clarity. The picture was captured at 12 ns. (F, G) Graph of RMSD and distance measurements of WT and MUT protein Cx26. (F) RMSD of the WT protein (black) and MUT protein (red). (G). Distance from Asp2 and Val37 in WT protein, and distance from Asp2 and Ile37 in the MUT protein. (H-K). Representation of Cx26 pore. (H) Hexagon formed by the α-carbons of the Asp2 amino acids of all subunits of the first hemichannel of Cx26. (I) The protein surface highlights the structure of the internal pores of the protein. Water, hydrogen, and the membrane were removed for clarity. Both figures were acquired at a simulation time of 23 ns. (J, K) Graphs represent the surface values of the pore during dynamics, with the x-axis indicating time in nanoseconds and the y-axis indicating the surface values in Å^2. The black and red lines represent WT and MUT, respectively. CAP-Gly, cytoskeleton-associated protein, glycine-rich; RMSD, root-mean-square deviation; WT, wild-type; MUT, mutated.

NH-terminal helix, while the paternal variant alters the first transmembrane helix, TM1 (Fig. 2E–G) leading to the pore closure and impaired ion passage (Fig. 2H and I).

The N-terminal CAP-Gly domain of TBCE interacts with the C-terminal EEY motif of α-tubulin, facilitating tubulin heterodimer assembly, essential for microtubule processes.[5] The rs767004810 in our patient disrupts this domain, likely impairing microtubule function and contributing to the phenotype. Prior studies showed similar effects where the channel's inner zone was restricted.[6] Surface area analysis confirmed that the pore of the wild-type *GJB2* remains open, while the mutant narrows, potentially leading to protein dysfunction and impaired intercellular communication (Fig. 2J and K). While *GJB2* variants are not typically associated with KCS1, they might influence the auditory deficits of our patient. In fact, both *GJB2* variants are candidate for molecular diagnosis of deafness.[7,8] Although TBCE and GJB2 have distinct roles—microtubule assembly and gap junction formation, respectively—both influence cytoskeletal dynamics. Since the interactors associated with the mutated TBCE protein in KCS1 have not been characterized, our PPI analysis aims to explore the potential interaction between *TBCE* and *GJB2* within a shared signaling pathway as it demonstrated at least under physiological state (Fig. 1). Comprehensive genetic screening in syndromic patients, especially those with atypical signs like hearing loss, may aid in personalized management. Considering that this study is based on a single patient, caution must be exercised in interpreting the results. The potential association between TBCE and GJB2 variants cannot be generalized to the broader population of KCS1 patients without further functional validation or confirmation in additional cases. Large studies should explore protein interactions between TBCE–GJB2 through cellular/animal models and track long-term outcomes in affected patients. Therefore, these findings should be considered as hypothesis-generating rather than conclusive.

The research was conducted ethically in accordance with the World Medical Association Declaration of Helsinki and approved by ethics committee of the University of Catania, Italy (Ethical Committee Catania 1 Clinical Registration no. 180/2023/PO).

Question

Which combination of clinical and biochemical features is most strongly suggestive of Kenny-Caffey syndrome type 1 in a newborn?

Answers:
(A) Macrocephaly, hypercalcemia, delayed fontanelle closure
(B) Microcephaly, hypocalcemia, dysmorphic features
(C) Hypotonia, hyperglycemia, hepatosplenomegaly
(D) Normal growth, hypoglycemia, facial angiomas

Correct answer: (B) Microcephaly, hypocalcemia, dysmorphic features

Footnotes

Supplementary material: Supplementary material 1 is available at https://doi.org/10.3345/cep.2025.00360.

Conflicts of interest: No potential conflict of interest relevant to this article was reported.

Funding: This study received no specific grant from any funding agency in the public, commercial, or not-for-profit sectors.

Author contribution: All authors contributed to the study conception and design. Material preparation, data collection and analysis were performed by MLB, FS, XGP, FF, GF, RR. The first draft of the manuscript was written by MLB and all authors commented on previous versions of the manuscript. All authors read and approved the final manuscript.

ORCID:
Manuela Lo Bianco https://orcid.org//0000-0002-5413-419X
Federica Sipala https://orcid.org/0000-0002-8477-3419
Xena Giada Pappalardo https://orcid.org/0000-0002-4640-6677
Gaia Fusto https://orcid.org/0009-0004-9498-8378
Roberta Rizzo https://orcid.org/0000-0003-1994-5218
Carla Cimino https://orcid.org//0000-0001-9032-7768
Silvia Marino https://orcid.org/0000-0001-6598-9903
Martino Ruggieri https://orcid.org/0000-0002-2658-4249
Agnese Suppiej https://orcid.org/0000-0001-5130-1450
Simone Ronsisvalle https://orcid.org/0000-0003-3488-7343
Raffaele Falsaperla https://orcid.org/0000-0002-4482-3506

References

1. Diaz GA, Gelb BD, Ali F, Sakati N, Sanjad S, Meyer BF, et al. Sanjad-Sakati and autosomal recessive Kenny-Caffey syndromes are allelic: evidence for an ancestral founder mutation and locus refinement. Am J Med Genet 1999;85:48-52.
2. Schigt H, Bald M, van der Eerden BC, Gal L, Ilenwabor BP, Konrad M, et al. Expanding the phenotypic spectrum of Kenny–Caffey syndrome. J Clin Endocrinol Metab 2023;108:e754-68.
3. Rak K, Frenz S, Radeloff A, Groh J, Jablonka S, Martini R, et al. Mutation of the TBCE gene causes disturbance of microtubules in the auditory nerve and cochlear outer hair cell degeneration accompanied by progressive hearing loss in the pmn/pmn mouse. Exp Neurol 2013;250:333-40.
4. Matthijs G, Souche E, Alders M, Corveleyn A, Eck S, Feenstra I, et al. Guidelines for diagnostic next-generation sequencing. Eur J Hum Genet 2016;24:2-5.
5. Serna M, Carranza G, Martín-Benito J, Janowski R, Canals A, Coll M, et al. The structure of the complex between α-tubulin, TBCE and TBCB reveals a tubulin dimer dissociation mechanism. J Cell Sci 2015;128:1824-34.
6. Zonta F, Buratto D, Cassini C, Bortolozzi M, Mammano F. Molecular dynamics simulations highlight structural and functional alterations in deafness-related M34T mutation of connexin 26. Front Physiol 2014;5:85.
7. Sydorchuk LP, Iftoda OM. New prognostic markers of hearing impairment in children: gene-gene interaction and approximation models. J Educ Health Sport 2020;10:373-81.
8. Liang S, Li W, Chen Z, Yuan S, Wang Z. Analysis of GJB2 gene mutations spectrum and the characteristics of individuals with c.109G>A in Western Guangdong. Mol Genet Genomic Med 2023;11:e2185.

How to cite this article: Lo Bianco M, Sipala F, Pappalardo XG, Fusto G, Rizzo R, Favata F, et al. Expanding genotype-phenotype correlation of Kenny-Caffey syndrome type 1. Clin Exp Pediatr 2025;68:616-9.